NG35B-0453

LEIBNIZ INSTITUTE OF ATMOSPHERIC PHYSICS IAP

Two-Dimensional Horizontal Correlation Functions in the MLT Region Estimated Using Multistatic Specular Meteor Radar Observations

F. Poblet[(1)], J. L. Chau[(1)], J. F. Conte[(1)], V. Avsarkisov[(1)], J. Vierinen[(2)] and H. Charuvil Asokan[(1,3)]

[(1)]Leibniz Institute of Atmospheric Physics at the University of Rostock, Kühlungsborn, Germany.

[(2)] University of Tromsø, Tromsø, Norway. [(3)] École Centrale de Lyon, Écully, France.

AGU FALL MEETING
New Orleans, LA & Online Everywhere
13–17 December 2021

Leibniz Association

Motivation

- The wind field correlation function inversion (WCFI) technique (Vierinen et al., 2019) is used to reconstruct 2D correlation functions, distributed in horizontal lags that cover the mesoscale range (tens to hundreds of km). The method is applied in the mesosphere and lower thermosphere (MLT) using specular meteor radar observations from the SIMONe 2018 campaign.
- With the velocity correlation tensor components (R'_{ij}) we can calculate other parameters, e.g. the correlation functions of the **vorticity tensor vertical component** (**Q_{zz}**) and the **horizontal divergence** (**P**) (Lindborg, 2007).
- The comparison between these two functions can provide information on the relative importance of stratified turbulence and internal gravity waves in the MLT.

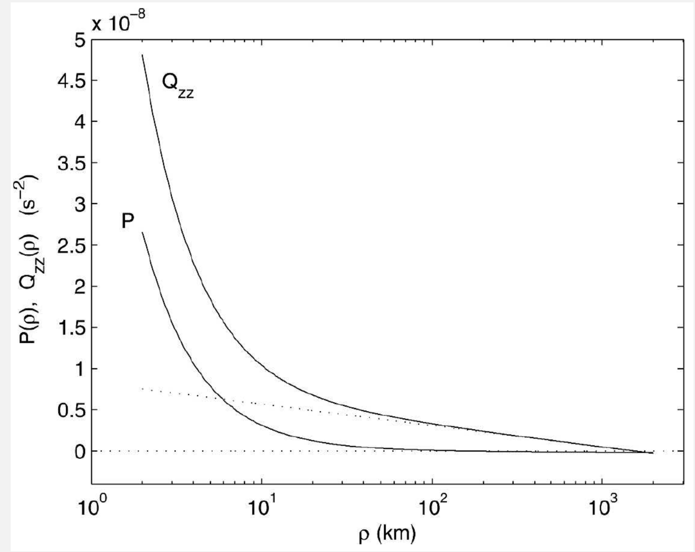

Original solution by Lindborg, (2007) in the UTLS

2D correlation functions determination

The determination of R'_{ij} is developed in two steps:

1. Meteor pairs selection procedure: (1) look for meteors separated no more than $\Delta\tau$ (temporal resolution), (2) the vertical separation of meteors must not exceed Δs_z (vertical resolution), (3) meteor pairs should be in the interval $\boldsymbol{s} \pm \Delta\boldsymbol{s}/2 = \left(s_x \pm \Delta s_x/2\,, s_y \pm \Delta s_y/2\right)$.
2. Solution of the linear system $\boldsymbol{y} = \boldsymbol{A}\,\hat{\boldsymbol{x}} + \boldsymbol{\eta}$. The system is formed by multiplying line-of-sight radial velocities ($r = 2\,\pi\, f = \boldsymbol{k}\cdot\boldsymbol{u} + \xi$) of two meteor pairs

$$4\pi^2 f_n f_m = (\mathbf{u}_n \cdot \mathbf{k}_n)\,(\mathbf{u}_m \cdot \mathbf{k}_m) + (\mathbf{u}_n \cdot \mathbf{k}_n)\,\xi_m + (\mathbf{u}_m \cdot \mathbf{k}_m)\,\xi_n + \xi_n\xi_m$$

considering every meteor pair and taking the expected value (the errors ξ are considered zero-mean, independent, and normally distributed random variables.)

Meteor-pair selection diagram for 2D R'_{ij}

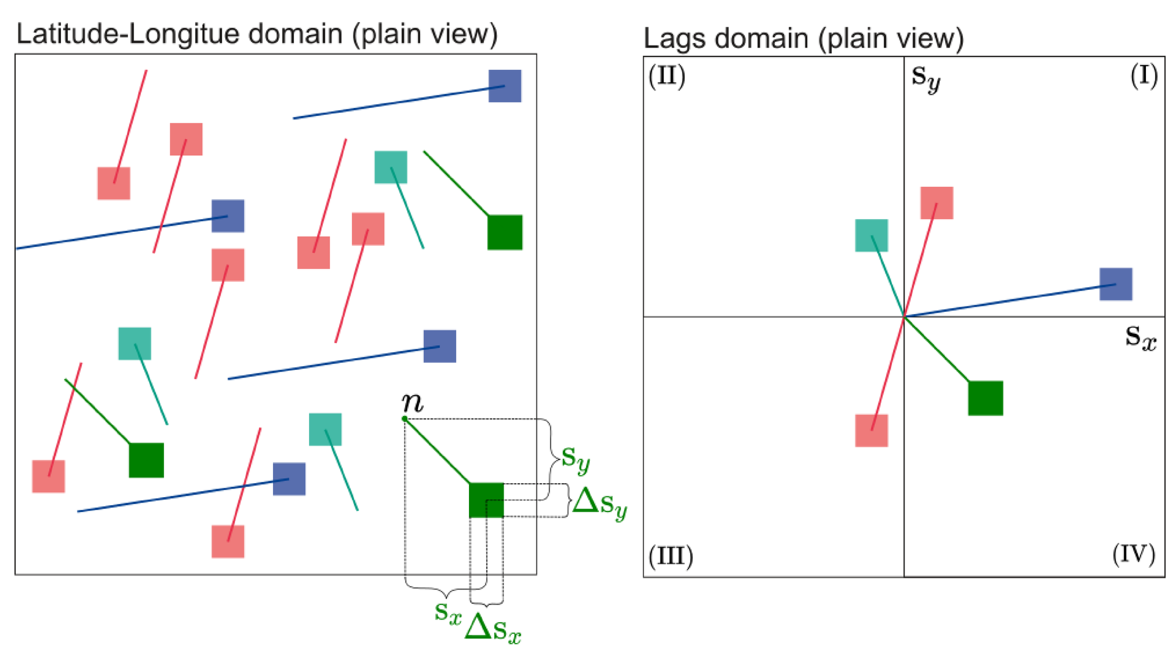

The solution is: $R'_{ij}(\mathbf{s}) = \langle u'_i(\mathbf{r})u'_j(\mathbf{r}+\mathbf{s})\rangle$.

Results

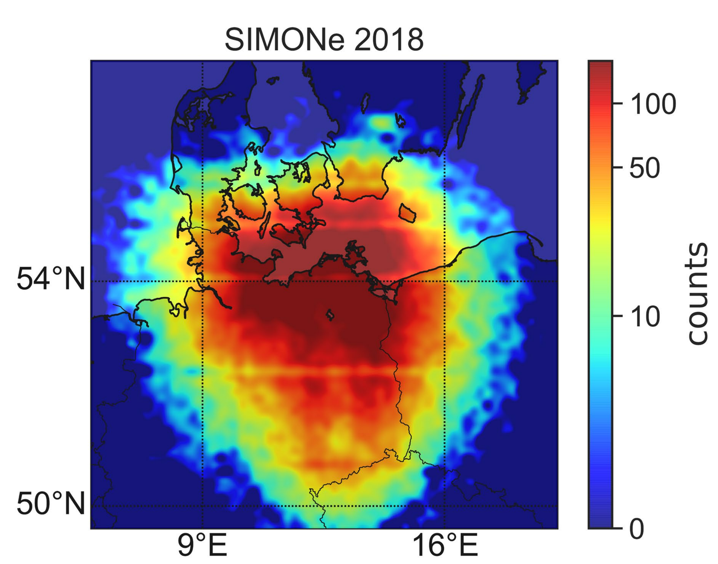

SIMONe 2018 data

- 7-day campaign in November 2018, conducted over northern Germany (Charuvil Asokan et al., 2021).
- A multistatic SMR approach was implemented: 14 multilinks, 8 of them new.
- ~10^5 meteor detections per day in a 500 x 500 km area of the MLT. This is **10 to 20 times** the amount of detections of monostatic SMRs.

2D zonal and meridional correlation functions

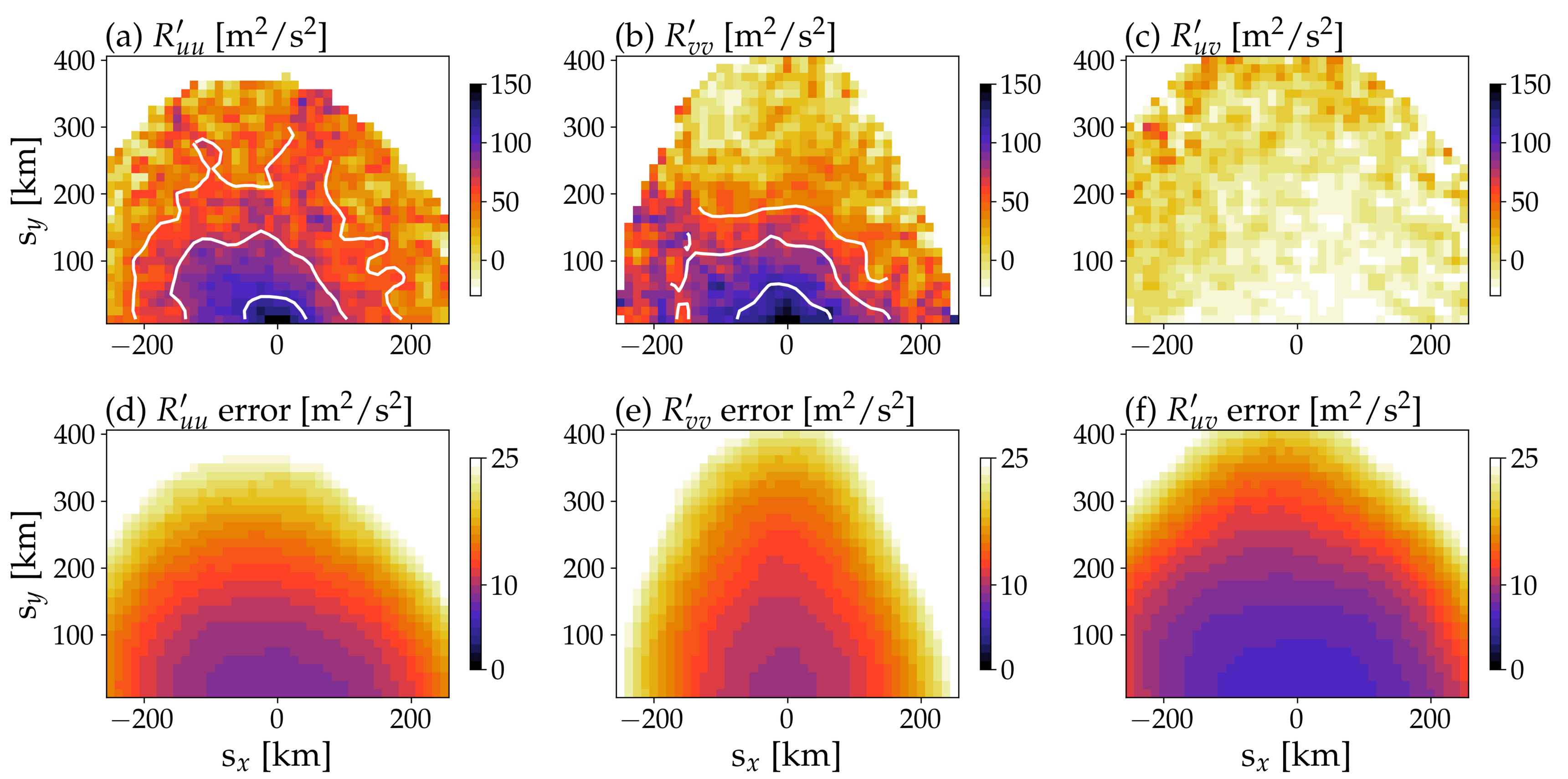

- Strong correlation values of R'_{uu} and R'_{vv} near the origin. They decrease as the distance from the origin increases.
- $R'_{uv} \simeq 0$ in the entire domain, i.e., **no preferential direction for the fluctuating wind during the campaign**. u and v are uncorrelated.
- The errors of the three components increase as the lag values grow.
- There are less number of pairs in longer lags to resolve the correlations.

Longitudinal and transverse correlation and structure functions

- To calculate Q_{zz} and P, we convert R'_{uu} and R'_{vv} to longitudinal (R'_{LL}) and transverse (R'_{TT}) components after applying WCFI, i.e., a post-statistics approach.
- The conversion relations (not just for fluctuating winds) are given by:

$$R_{LL}(\mathbf{s}) \simeq R_{uu}(\mathbf{s})\cos^2\phi + R_{vv}(\mathbf{s})\sin^2\phi,\;\; R_{TT}(\mathbf{s}) \simeq R_{uu}(\mathbf{s})\sin^2\phi + R_{vv}(\mathbf{s})\cos^2\phi$$

under the condition $|\Delta\mathbf{s}| < |\mathbf{s}|$

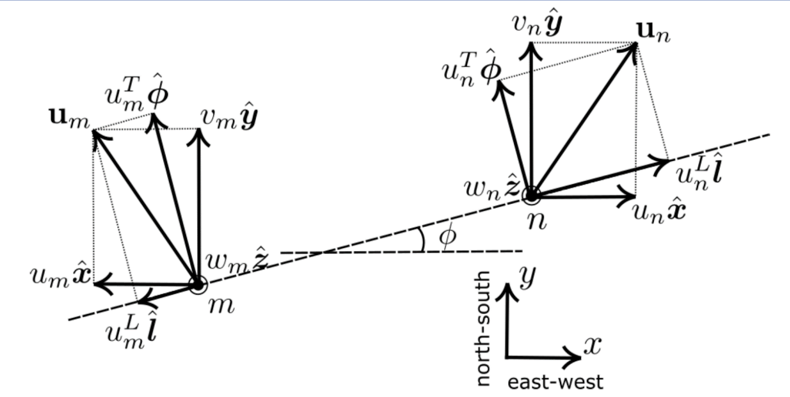

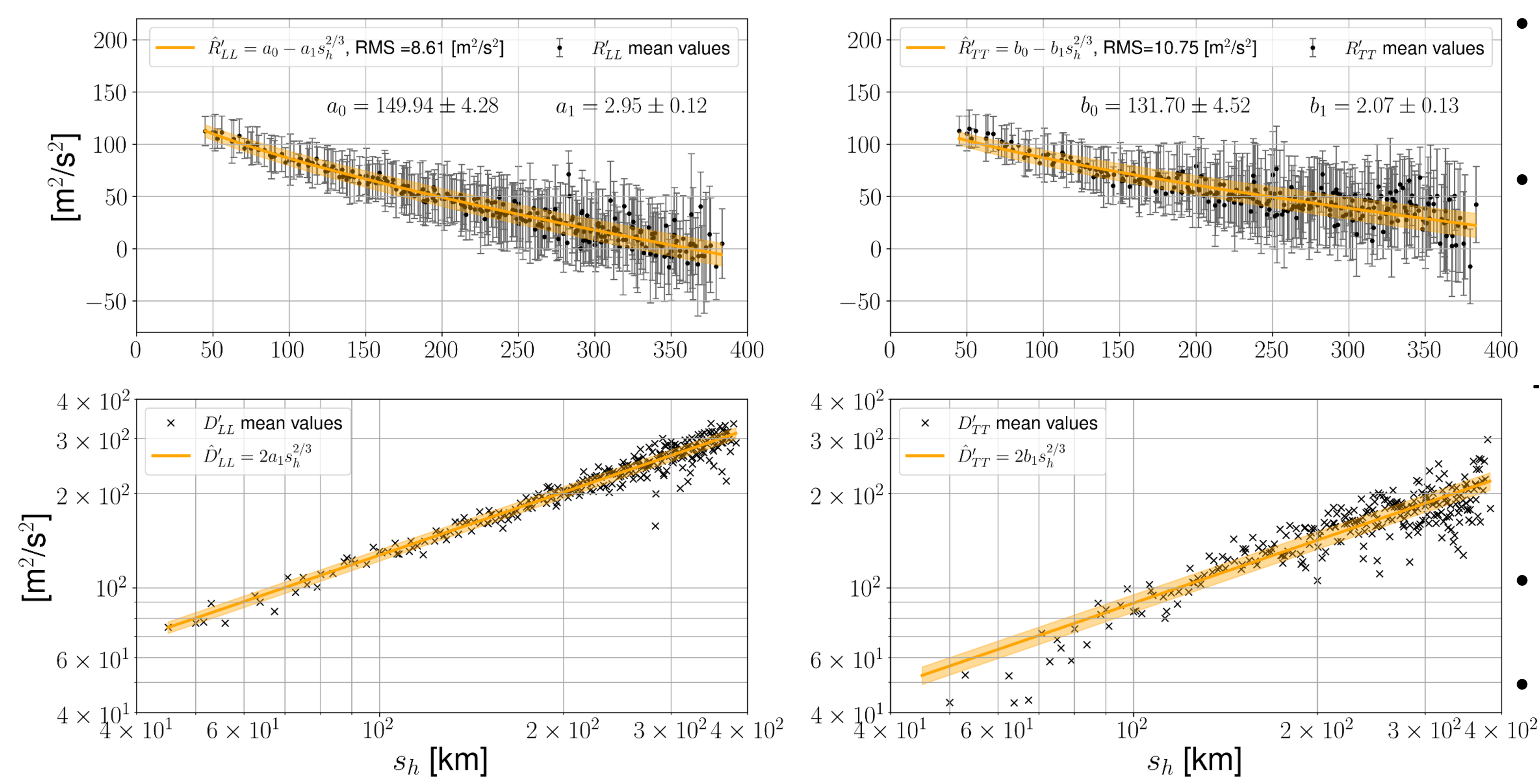

- A 2/3-power law is used to fit the observations (-5/3 exponent in wavenumber domain).
- R'_{TT} shows a longer decorrelation distance than R'_{LL}. For R'_{LL}, this distance is $s_h \simeq \sqrt{s_x^2 + s_y^2} \simeq 360$ km.

The **structure functions** can be determined as:

$$D'_{LL} = 2\,(a_0 - R'_{LL})$$
$$D'_{TT} = 2\,(b_0 - R'_{TT})$$

- Remarkable agreement of D'_{LL} with a 2/3-power function.
- D'_{TT} shows larger dispersion but the 2/3-power law is still a good approximation.

Vertical vorticity and horizontal divergence correlation functions and spectra

The vorticity tensor (Q_{ij}) and horizontal divergence (P) correlation functions are defined as (Lindborg, 2007):

$$Q_{ij}(\boldsymbol{s}) = \langle\zeta_i(\boldsymbol{r})\zeta_j(\boldsymbol{r}+\boldsymbol{s})\rangle; \quad \boldsymbol{\zeta} = \nabla_{\boldsymbol{r}} \times \boldsymbol{u}' \qquad P = \langle(\nabla_h \cdot \boldsymbol{u}'_h(\boldsymbol{r}))(\nabla_h \cdot \boldsymbol{u}'_h(\boldsymbol{r}+\boldsymbol{s}))\rangle$$

Assuming homogeneity and horizontal isotropy, P and the vertical component of Q_{ij} are

$$Q_{zz}(s_h) = \frac{1}{s_h}\frac{\partial R'_{LL}(s_h)}{\partial s_h} - \frac{1}{s_h^2}\frac{\partial}{\partial s_h}\left(s_h^2\frac{\partial R'_{TT}(s_h)}{\partial s_h}\right);$$
$$P(s_h) = \frac{1}{s_h}\frac{\partial R'_{TT}(s_h)}{\partial s_h} - \frac{1}{s_h^2}\frac{\partial}{\partial s_h}\left(s_h^2\frac{\partial R'_{LL}(s_h)}{\partial s_h}\right)$$

Comparison between these two quantities can shed light on the relative importance of stratified turbulence and internal gravity waves.

Replacing the correlation fits into these expressions, yields:

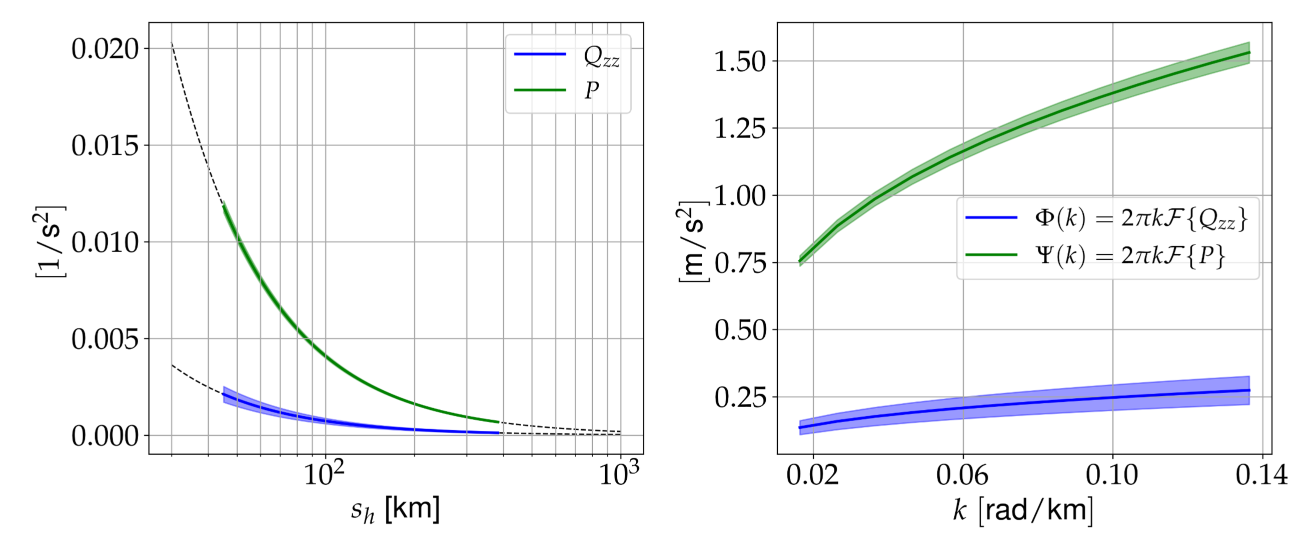

$$Q_{zz} = q_1 s_h^{-4/3}, \qquad P = p_1 s_h^{-4/3}$$

With

$$q_1 = \tfrac{2}{3}\left(\tfrac{5}{3}b_1 - a_1\right) = 0.34\times10^{-2}\mathrm{m}^{4/3}\mathrm{s}^{-2}$$
$$p_1 = \tfrac{2}{3}\left(\tfrac{5}{3}a_1 - b_1\right) = 1.90\times10^{-2}\mathrm{m}^{4/3}\mathrm{s}^{-2}$$

Divergent modes predominance during the SIMONe 2018 campaign

Selected references

- Vierinen et al. (2019). Observing mesospheric turbulence with specular meteor radars: A novel method for estimating second-order statistics of wind velocity. EES.
- Lindborg (2007). Horizontal Wavenumber Spectra of Vertical Vorticity and horizontal Divergence in the Upper Troposphere and Lower Stratosphere. JAS.
- Charuvil Asokan et al. (2021). Frequency spectra of horizontal winds in the mesosphere and lower thermosphere region from multistatic specular meteor radar observations during the SIMONe 2018 campaign. Under review in EPS.
- Poblet et al. (2021). Horizontal wavenumber spectra of vertical vorticity and horizontal divergence in the mesosphere and lower thermosphere using multistatic specular meteor radar observations. To be submitted.